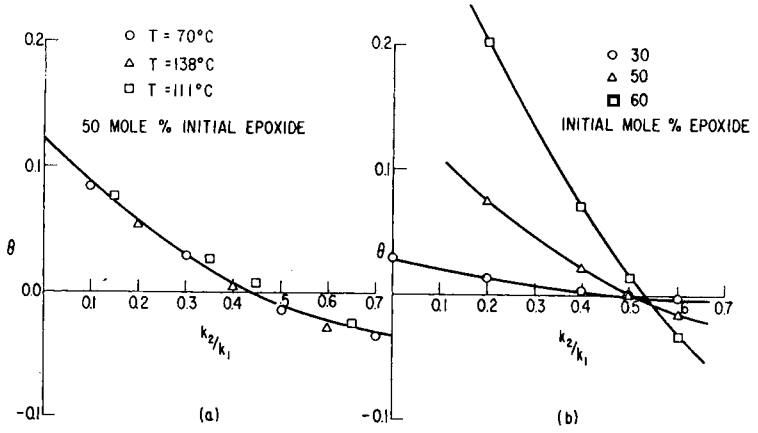

Fig. 1. Propylene oxide–butylamine reaction. Plots of θ versus k_2/k_1 for the function

$$\theta = k_2/k_1 \log (B_\infty/B_0) - \log \{(B_\infty/B_0) + (C_\infty/B_0)(1 - k_2/k_1)\}.$$

siderable problems in chemical and kinetic analysis.[2] Although the three-step reaction of ammonia with epoxides is inevitably mathematically complex, the two-step reaction of primary amines can be treated fairly simply.

For the reactions:

$$A + B \xrightarrow{k_1} C \quad (1)$$

$$A + C \xrightarrow{k_2} D \quad (2)$$

$$-d[C]/d[B] = 1 - \alpha[C]/[B] \quad (3)$$

where $\alpha = k_2/k_1$.

Solution of this equation yields

$$\alpha \ln \frac{[B]}{[B_0]} = \ln \{[B]/[B_0] + ([C]/[B_0])(1 - \alpha)\} \quad (4)$$

where $[B_0]$ is the initial concentration of [B] and the other concentration terms refer to any time throughout the course of the reaction. The same result may be obtained by using the "static" treatment of Fuoss.[3] Since this equation holds for the complete course of the reaction, it should be possible to evaluate α from measurements of [B] and [C] after the reaction has virtually gone to completion.

We have applied this treatment to the reaction of propylene oxide with *n*-butylamine, where a series of different substoichiometric amounts of propylene oxide reacted in Carius tubes with butylamine to virtual completion. The reaction products were analyzed by vapor phase chromatography on a 2-ft. silicone rubber column programmed at 7.9°C./min. and starting at 80°C. Under these conditions the three end products were well separated and their mole fractions calculated from calibration curves obtained with mixtures of known composition.

The results of several experiments at different compositions and temperatures are shown in Figure 1. From eq. (4) it can be seen that the intercepts $\theta = 0$ in Figure 1 represent the true values of k_2/k_1.

It can readily be seen that k_2/k_1 is virtually independent of temperature and composition over a considerable range of both, and has a value of 0.49 ± 0.05. It is expected that this figure will be fairly independent of the substituents on either reactant for the epoxide–primary amine reaction, and the value of 6:4 obtained by Potter and McLaughlin[2] for the competition of mono- and diethanolamine for ethylene oxide supports this contention.

Extrapolating these conclusions to primary amine-cured epoxy resins, one may conclude that gelation should generally occur at higher conversions than those predicted by the Flory-Stockmayer[4] theory because of the unequal activity of the amine functions. Second, the branching coefficient should be independent of temperature. This means there should be no temperature-dependent chemical influence on the structure of the network. The possibility of temperature-dependent physical influences is, of course, considerable.

The author would like to thank Dr. H. A. Dewhurst for use of chromatographic equipment.

References

1. Smith, I. T., *Polymer*, **2**, 95 (1961).
2. Potter, C., and McLaughlin, R. R., *Can. J. Res.*, **25B**, 405 and 415 (1947).
3. Fuoss, R., *J. Am. Chem. Soc.*, **65**, 2406 (1943).
4. Flory, P. J., *Principles of Polymer Chemistry*, Cornell Univ. Press, 1953, p. 353.

JOHN F. HARROD

General Electric Research Laboratory
Schenectady, New York

Received September 20, 1961

Water Vapor Transmission Through Porous Films

The usefulness of porous plastic films in many applications—for example, wearing apparel—depends to a large degree on their capability of transmitting water vapor. The variety of commercially available porous plastic sheets and films is increasing, while the methods of evaluating water vapor transmission of such films leave much to be desired. In general, water vapor transmission rates (WVTR) are measured by placing a sample between two layers of air at different humidities. The comparison of data obtained

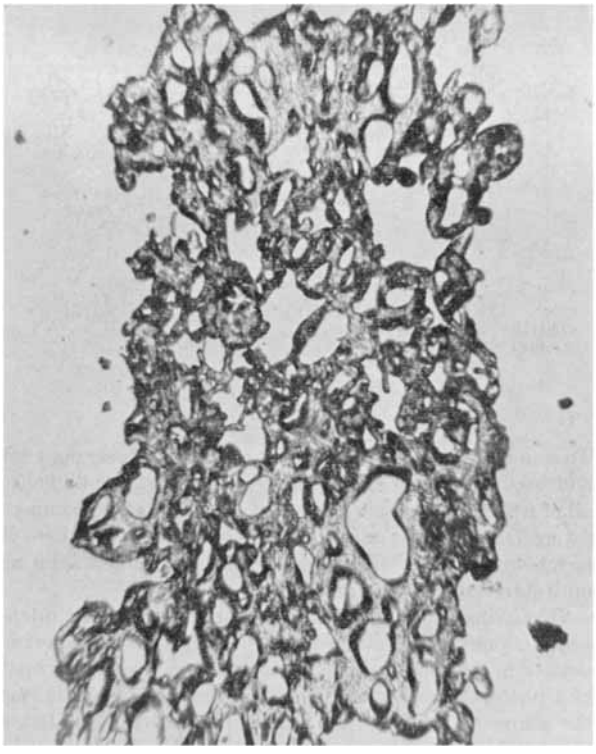

Fig. 1. Cross section of a 40-mil type A porous poly(vinyl chloride) sheet. 58×.

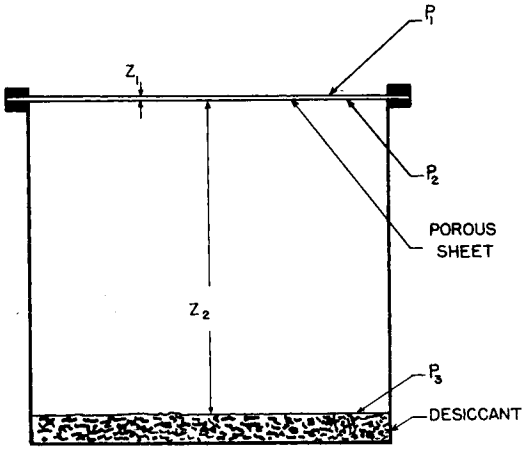

Fig. 2. Thwing-Albert Vapometer cup.

under different test conditions, i.e., temperature, sample container, varying relative humidities, is difficult.

It is believed that water vapor transmission in plastic sheets with interconnected air-filled pores takes place primarily by gas phase molecular diffusion. The analysis of experimental data presented in this note is based on this assumption. The introduction of basic gas diffusion principles may help to develop a more general method for the evaluation of WVTR. The effect of area available for diffusion and tortuosity of the passages in porous film is accounted for by the constant K, which is deduced from the diffusion data.

WVTR of porous poly(vinyl chloride) sheets (Fig. 1) was investigated. Samples were die cut to fit a cylindrical Thwing-Albert Vapometer cup, 5.4 cm. high by 6.35 cm. in diameter (Fig. 2). The cups were filled with a desiccant (LiCl) to a level of 0.6 cm. and the sample was secured to the cup. The assembly was placed in a constant-temperature constant-humidity atmosphere and the cup assembly was periodically weighed. The data used for WVTR determination were taken after the establishment of steady-state conditions, ascertained by constant rate of gain in weight.

Assuming water vapor is transferred by molecular diffusion, eq. (1) for steady-state diffusion of one gas through a second stagnant gas should apply:[1]

$$N_w = (DP/RTp_a)(dp_a/dz) \quad (1)$$

Upon integration:

$$N_w = (DP/RTz)(p_{w1} - p_{w2})/p_{am} \quad (2)$$

where

$$p_{am} = (p_{a2} - p_{a1})/\ln (p_{a2}/p_{a1})$$

N is the rate of diffusion, D is the gaseous diffusion coefficient, P is the total pressure, p is the partial pressure of one component, R is the gas law constant, and z is the linear distance in the direction of diffusion. The subscripts "w" and "a" denote water vapor and air respectively.

In place of a porous plastic sheet in the actual system shown in Figure 2, a hypothetical film is assumed which has no resistance to molecular diffusion and is only a barrier to eddy diffusion. WVTR as a function of water vapor pressure differential is calculated from eq. (3) for this hypothetical system and is graphically represented by curve 1 in Figure 3.

$$N_w = DP/RTz_2[(p_{w1} - p_{w3}) \ln (p_{a3}/p_{a1})]/(p_{a3} - p_{a2}) \quad (3)$$

Curve 2 is constructed from experimental results obtained in an actual system for the determination of WVTR through a porous plastic sheet. A horizontal line drawn from any point of curve 2 is divided into two parts by curve 1. Δp_S represents the driving force across the sample and Δp_L the driving force across the stagnant layer of air. The value of water vapor pressure at the intersection of the horizontal

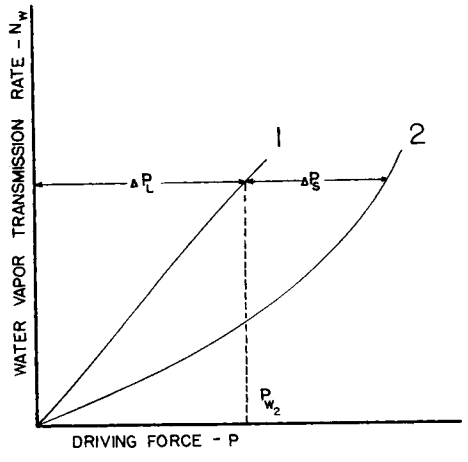

Fig. 3. Graphic method of obtaining the water vapor pressure p_{w_2} at the sample–stagnant air layer interface.

line and curve 1 is the pressure p_{w2} at the sample–air interface. After p_{w2} is determined, K can be calculated from eq. (4):

$$N_w = K\,DP/RTz_1$$

$$[(p_{w1} - p_{w2})\ln(p_{a2}/p_{a1})]/(p_{a2} - p_{a1}) \quad (4)$$

Where z_1 is the film thickness and K is a dimensionless parameter representing the ratio of the fraction of cross-sectional area available to diffusion to the tortuosity of the passages.

K obtained in this manner should be independent of test conditions, i.e., humidity, temperature, and the height of the air layer between the desiccant and the sample. Table I shows K calculated from the limited amount of experimental data taken at various water vapor pressures.

TABLE I
Values of K at Various Water Vapor Pressures

Water vapor pressure, mm. Hg	K	
	Material A at 90°C.	Material B at 67°C.
50	—	0.0226
100	0.0193	0.0242
150	—	0.0275
200	0.0189	
300	0.0178	
400	0.0188	

We thank Dr. J. H. Hollister for his helpful discussion.

Reference

1. Sherwood, T. K., and R. L. Pigford, *Absorption and Extraction*, McGraw-Hill, New York, 1952, p. 5.

Donatas Satas
Donald G. Carr

Chicago Division Research Laboratories
The Kendall Company
Chicago, Illinois

Received October 16, 1961

Optical Transducer for Detecting Resonant Frequency and Free-End Amplitude of a Vibrating Reed (Low Driving Force)

In the vibrating reed or resonance method of mechanical dynamic testing the amplitude of vibration, as related to frequency, at the free end of the reed is a variable that is difficult to measure accurately. In one method of mechanical dynamic testing[1] the reed's free-end amplitude is measured at reed resonance and at discrete frequency increments above and below resonance. The transducer described in this note was designed to meet the above requirements. While inductance,[2] capacitance,[3] and optical transducers[4] have been successfully used for this work, the optical transducer has certain inherent advantages in regard to the detection of the free-end vibration of a reed.

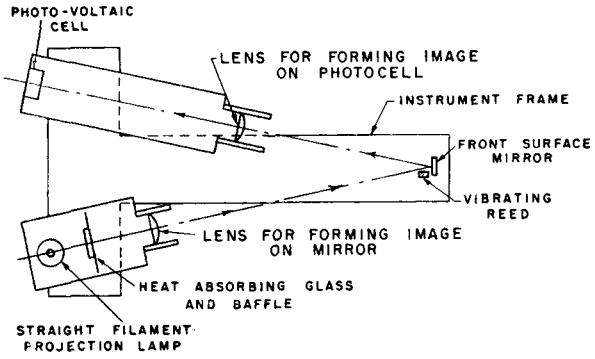

Fig. 1. Diagram of optical system.

To sum up these advantages, the optical transducer does not add friction or mass and/or electrostatic or magnetic fields, all of which are possible sources of error and add a compensating factor to the measurements. In contrast, there is never any "factor" to be added to or subtracted from an optical transducer measurement.

Shadowing or occluding a light source of constant intensity is an obvious and widely used method of photoelectric detection. As an example, a method of varying the output of a photocell employing a shaped aperture and shadowing the source of incident light was employed by B. G. Leary in a study of textile yarns.[5] On the other hand, a light intensity change of the source illumination also has an intrinsic advantage. The transducer described herein is a combination of these two approaches to photoelectric detection.

Essentially, the techniques employed in the design of this transducer consist of focussing a magnified image of a straight filament tungsten projection lamp onto a front surface mirror which in turn reflects the light of this image back toward a photovoltaic cell. Some degree of image magnification for the lamp filament is desirable, but the actual amount strictly is arbitrary. A second lens is used to focus an image of the illuminated front surface mirror onto the photo cell. In this case the magnification might just as well be unity for practical purposes. The filament image acts as the source of light for the photo cell and the light of this image is occluded by the reed sample. Since the edges of the filament image are irregular, the light return mirror is made to a definite rectangular shape, the long side of the rectangle being parallel to the filament. The mirror area is smaller than the image area, thus eliminating the fuzzy edges and giving a geometrically precise light source for the photocell to look at. This arrangement is analogous to a brightly illuminated slit, with the advantage that the projector and photocell are on the same side of the vibrating sample. The apparatus is illustrated in Figure 1.

In use, the light from the filament image is periodically occluded by the vibrating reed, resulting in corresponding light intensity change on the photocell. In this particular instance the occlusion is sinusoidal; therefore the photocell response will be sinusoidal. The photocell output is put into a sensitive oscilloscope. The oscilloscope trace will accurately show the resonant point of the reed. The free-end amplitude can be measured if the system is calibrated; also, frequency can be measured, depending on the characteristics of the oscilloscope.